Lung involvement by chest CT images in covid-19 patients in a Specialty Hospital in the Northeast of Mexico

Afectación pulmonar mediante imágenes de TC de tórax en pacientes con covid-19 en un Hospital de Especialidades del Noreste de México

Francisco Javier García-Alvarado[1*], Melisa Alejandra Muñoz Hernández[1], Fany Karina Segura Lopez[1], Héctor Alberto Delgado-Aguirre[1], Yazmín Esmeralda Gaona Hernández[2], Jaime Suriel Arellano Rosales[2]

1 Department of Health Research, Instituto Mexicano del Seguro Social (IMSS), Unidad Médica de Alta Especialidad (UMAE) No. 71, Torreón, Coahuila, México. Código postal: 27240 Teléfono: 871 729 0800. Correo electrónico: ibqjaviergarcia01@gmail.com. ORCID: Francisco Javier García-Alvarado: 0000-0002-3760-1876. Héctor Alberto Delgado-Aguirre: 0000-0001-5448-7975
2 Department of Radiology, Computed Tomography (CT),Instituto Mexicano del Seguro Social (IMSS), Unidad Médica de Alta Especialidad (UMAE) No. 71, Torreón, Coahuila, México.
*Corresponding author

Abstract

Chest imaging (CT) plays an important role in the detection and diagnosis of covid-19. The objective of this study is the local experience of CT-based semi-quantitative score of lung involvement as well as the clinical staging in covid-19 patients at the Specialty Medical Institution No. 71 (UMAE, from its Spanish acronym). This is a single-center, retrospective study, in which 71 patients (44 men, 27 women; mean age 50 ± 14.1, range 25-84 years) were selected with positive tests of RT-PCR for SARS-CoV-2 and a confirmed diagnosis of covid-19. Chest CT images showed as predominant pattern the mixed pattern ($n = 26$, 36.6%), and other common findings included ground glass opacities (GGO) ($n = 25$, 35.2%), crazy paving ($n = 15$, 21.1%), and lung consolidation ($n = 5$, 7.0%). The chest computed tomography findings were bilateral lesions ($n = 64$, 90.1%), subpleural distribution ($n = 61$, 85.9%), and lower lobes ($n = 31$, 43,6%). The characteristic pulmonary tomographic pattern was ground-glass opacities and a bilateral mixed pattern of peripheral distribution towards the posterior regions.

Keywords: Chest computed tomography; SARS-CoV-2; clinical.

Resumen

La imagen de tórax (TC) tiene un papel importante en la detección y diagnóstico de covid-19. El objetivo de este estudio es la experiencia local de la puntuación semicuantitativa de la afectación pulmonar basada en la TC, así como la estadificación clínica en pacientes con covid-19 en la Unidad Médica de Alta Especialidad N° 71 (UMAE). Se trata de un estudio retrospectivo unicéntrico, en el que se seleccionaron 71 pacientes (44 hombres, 27 mujeres; edad media 50 ± 14.1, rango 25-84 años) con pruebas positivas de RT-PCR para SARS-CoV-2 y diagnóstico confirmado por covid-19. Las imágenes de TC de tórax mostraban como patrón predominante el patrón mixto ($n = 26$, 36.6%), y otros hallazgos comunes incluían opacidades en vidrio esmerilado (GGO, por sus siglas en inglés) ($n = 25$, 35.2%), el patrón de *crazy paving* ($n = 15$, 21.1%) y consolidación pulmonar ($n = 5$, 7.0%). Los hallazgos de la tomografía computarizada de tórax fueron lesiones bilaterales ($n = 64$, 90.1%), distribución subpleural ($n = 61$, 85.9%) y lóbulos inferiores ($n = 31$, 43.6%). El patrón tomográfico pulmonar característico fue opacidades en vidrio esmerilado y un patrón mixto bilateral de distribución periférica hacia las regiones posteriores.

Palabras clave: Tomografía computarizada de tórax; SARS-CoV-2; clínica.

Background

The coronavirus disease 2019 (covid-19) pandemic caused by the severe acute respiratory syndrome coronavirus 2 (SARS-CoV-2) has resulted in serious economic problems and mortality worldwide (World Health Organization [WHO], 2020a). The WHO declared this pathology as a global public health emergency on January 30th, 2020 and communicated the first case in Latin America approximately one month later (Sánchez-Duque *et al.*, 2020). The first case reported with covid-19 in Mexico was detected on the 27th of February 2020.The state of Coahuila announced the first case of SARS CoV-2 infection two days later. On March 30th, a public health emergency was decreed in the country (Suárez *et al.*, 2020).

Chest imaging (CT) is an appropriate method to detect and manage these patients, which has been employed for diagnosis, determination of disease severity, guiding treatment, and assessment of therapeutic response; high-resolution CT is extensively applied for early diagnosis of covid-19. High-resolution chest CT technology, as a rapid test with a sensitivity of 97%, is now regarded as the most sensitive imaging test to detect covid-19 (Ai *et al.*, 2020). In addition, it is also applicable as a follow-up method for monitoring disease progression and assessing the covid-19 severity (Jiang *et al.*, 2020).

The most common chest computed tomography (CT) findings in covid-19 pneumonia include ground-glass; consolidated, cobblestone or crazy paving opacity; solid nodules; prominent peripheral subpleural distribution; and a preferential predilection for the posterior or lower lobe (Zu *et al.*, 2020). Ground glass opacities (GGO) distributed bilaterally with or without consolidation in the posterior and peripheral lungs can be considered as the most specific and basic findings of covid-19 (Chung *et al.*, 2020; Wang *et al.*, 2020). Some CT findings might be more prevalent in severe and deceased covid-19 patients than non-severe patients (Prokop *et al.*, 2020). However, with subsequent analysis of the increasing number of cases, heterogeneity of features on CT images, including lining opacity, pleural effusion, lymphadenopathy, and inverted halo sign, among others, was observed (Bernheim *et al.*, 2020), which can indicate the possible mechanism behind the lung damage in covid-19.

The covid-19 clinical spectrum appears to be broad, including mild upper respiratory tract disease, asymptomatic infection, and severe pneumonia with respiratory failure; the specific information characterizing moderate to critical grade patients remains unclear. Also, the lack of reproducibility and the results of different analyses of tomographic and covid-19 imaging findings performed by different investigators are inconsistent.

Given the above, chest CT has been considered a fundamental part of the diagnostic process for SARS-CoV-2 lung involvement because of its high sensitivity; it could be a useful tool to assess the temporality of SARS-CoV-2 infection. Chest CT is helpful for stratifying the disease clinical stage. The current study aimed at describing the chest CT and the lung involvement of patients infected with SARS-CoV-2 in a Specialty Hospital of the Northeast Region of Mexico.

Materials and Method

Study design and participants

This single center retrospective research was conducted on a cohort (*n* = 315) of symptomatic patients suspected to have covid-19 pneumonia from November 15th, 2020, to February 2nd, 2021. Seventy-one patients who met the criteria for a confirmed case of covid-19 were selected and underwent chest CT scans at the diagnostic and therapeutic imaging unit of the High Specialty Medical Unit. The unit's ethics and research committee approved this study with registration number R-2021-501-020.

ISSN online 2007-9621

García-Alvarado, F. J., Muñoz Hernández, M. A., Segura Lopez, F. K., Delgado-Aguirre, H. A. Gaona Hernández, Y. A., & Arellano Rosales, J. S.
Lung involvement by chest CT images in covid-19 patients in a Specialty Hospital in the Northeast of Mexico | 1-12

Covid-19 Diagnostics

The confirmation of the covid-19 positive cases was carried out by the polymerase chain reaction in real-time according to the WHO criteria (WHO, 2020b).

Covid-19 classification according to the severity of symptoms

According to the severity of their symptoms, subjects were classified into three groups of covid-19 patients (moderate, severe, and critical) in accordance with the guidelines to diagnose and treat the covid-19, published by the National Health Commission of China (Wu & McGoogan, 2020). Subsequently, chest CT scans were performed in the Radiology and Imaging Department of the High Specialty Medical Unit. The patients selected for the study underwent a thin-section CT scan at least once. The clinical parameters were obtained from the electronic medical records of the hospital.

Acquisition of chest CT images

A non-contrast chest CT scan was performed while the subject was lying in supine position, considering a scan at the end of inspiration. To minimize motion artifacts, patients were instructed on how to hold their breath. The studies were performed on a 64-slice multiple detector tomograph (Revolution EVO, GE Healthcare, Milwaukee, WI, USA) Toshiba Activion 16 (Japan). Axial images were taken considering the following parameters: section thickness: 1mm; interval: 1.25 mm; and with adaptive tube current at 120 kVp. The reconstructed images were transmitted to the workstation for processing the multiplanar, sagittal, and coronal reconstructions for evaluation.

Analysis of CT scans and study image interpretation

The analysis and interpretation of the tomographic images were performed by two radiologist specialists assigned to the hospital's diagnostic and therapeutic imaging unit, who were blinded to the results of RT-PCR and clinical data of each patient. Definitions of radiological terms such as GGO, crazy paving, and pulmonary consolidation were according to an accepted glossary for thoracic imaging published by the international standard nomenclature, introduced by the Fleischner Society Glossary (Hansell *et al.*, 2008), and recently published studies on viral pneumonia (Ooi *et al.*, 2004).

Semi-quantitative measurement of the extent of lung lobe lesions

According to the method described by Pan *et al.* (2020), the semi-quantitative CT severity score of patients was determined for all lobes, as follows: 0, lack of involvement; 1, involvement of lower than 5%; 2, 5%-25% involvement; 3, 26%-50% involvement; 4, 51%- 75% involvement; and 5, involvement of more than 75%; the maximum total score was 25. The final score is interpreted as follows: mild impairment, 1 to 5 points; moderate impairment, > 5 to 15 points; and severe impairment, > 15 points. When data were present, some related characteristics, like subpleural lines, fibrosis, pleural effusion, inverted halo sign, and lymphadenopathy, were defined as well.

Statistical analysis

Qualitative variables were expressed using frequencies and percentages, whereas mean, standard deviation, and interquartile range were used to express the quantitative variables. The chi-square test (x^2), Fisher's exact test, and student t-test were used to compare the mean values using STATA 16 (Stata Corp LLC, College Station, Texas, EE. UU); a $p \leq 0.05$ was regarded statistically significant.

Results

Seventy-one patients who had a positive RT-PCR test for SARS CoV-2 (44 male and 27 female patients; mean age 50 ± 14.1; range: 25–84 years) were studied. The highest proportion of patients (47.8%) was found in an age range of 51–85 years. The patients presented a mean body mass index of 27.9 kg/m^2, of which 19 individuals were obese. Among the population studied, the largest proportion of patients had a history of at least one comorbidity, 13 (18.3%) suffered from systemic arterial hypertension, and 10 (14.1%) suffered from diabetes mellitus, being obesity the most frequent with 26.7%.

The most frequent symptomatology was fever, which was present in 55 (77.4%) of the patients, followed by dyspnea (60.5%), cough (53.5%), and headache (23.9%), among other less frequent symptoms. Oxygen saturation (SaO2) on admission averaged 91% with a PaO2/FiO2 ratio of 86. The median follow-up duration was 14 days (range: 5–31 days) from admission, and the duration of disease from the onset of symptoms to discharge from the hospital death or the end of the study was 22 days (range: 10–36).

During hospitalization, there were some significant laboratory findings; for instance, a decrease in lymphocyte levels was observed with an average concentration of 1.4 ± 0.3 and leukocytes of 8 ± 1.5. Regarding inflammatory mediators, an increase was found in D-dimer levels with an average of 625.4 ± 61.3. Table 1 presents demographic information, symptoms, and clinical parameters.

Table 1. General characteristics of patients infected with SARS-CoV-2.

features	Positive patients (+) SARS-CoV-2	
	n = 71	
Sex, no. of patients/ (%)		
Female	27	(38.0%)
Male	44	(61.9%)
Age range, no. of patients/ (%)		
	mean (SD $\pm$)	
Age	50 $\pm$ 14.1	
0-25	4	(5.6%)
26–50	33	(46.4%)
51–85	34	(47.8%)
	mean (SD $\pm$)	
weight (kg)	74.6 $\pm$ 6.1	
size (m)	1.6 $\pm$ 0.6	
BMI	27.9 $\pm$ 2.5	
Symptoms no. of patients /(%)		
Fever	55	(77.4%)
Dyspnea	43	(60.5%)
Cough	38	(53.5%)
Headache	17	(23.9%)
Clinical and laboratory findings		
	mean (SD $\pm$)	
White blood cells $\times 10^9$ cells/L	8 $\pm$ 1.5	
Lymphocytes $\times 10^9$ cells/L	1.4 $\pm$ 0.3	
D-dimer $^{ng/mL}$	625.4 $\pm$ 61.3	
Oxygen saturation (SaO^2)	89 $\pm$ 3.5	
Ratio PaO ^{2} / FiO ^{2}	86 $\pm$ 4.2	
Comorbidities, no. of patients/ (%)		
Diabetes	10	(14.1%)
Hypertension	13	(18.3%)
Obesity	19	(26.7%)

Source: Authors' own elaboration.

According to the tomographic findings (Figure 1), the predominant pattern was the mixed pattern (n = 26, 36.6%), and other common findings included ground glass pattern (GGO) (n = 25, 35.2%), followed by the crazy pattern paving (n = 15, 21.1%) and pulmonary consolidation (n = 5, 7.0%). Some of the related characteristics of the chest tomography were found as follows: subpleural lines (n = 25, 35.2%), lymphadenopathy (n = 20, 28.1%), fibrosis (n = 13, 18.3%), pleural effusion (n = 11, 15.4%), and inverted halo sign (n = 2, 2.8%). Pulmonary tomographic lesions were found with higher frequency bilaterally (n = 64, 90.1%), subpleural distribution (n = 61, 85.9%), and in the lower lobes (n = 31, 43.6%) (Table 2).
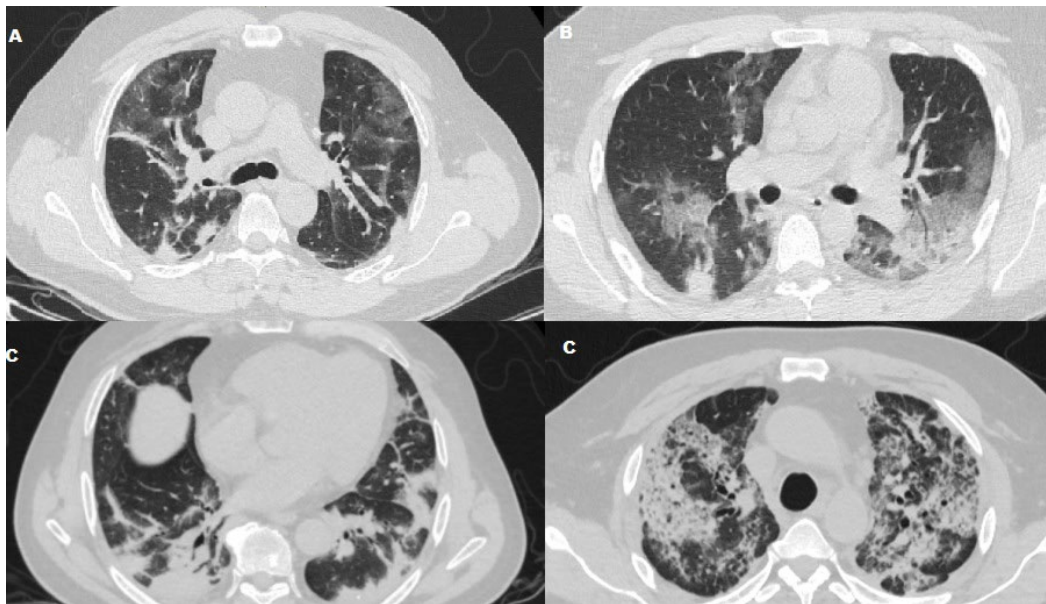

Figure 1. Chest computed tomography findings. a) Ground glass opacity; b) Crazy paving; c) Consolidation.

Table 2. Findings in thoracic computed tomography imaging in covid-19 patients.

CT-Scan findings	$n = 71$	%
Tomographic pattern		
Ground glass opacity	25	35.2
Crazy paving	15	21.1
Consolidation	5	7.0
Mixed	26	36.6
localization		
Unilateral	7	9.9
Bitateral	64	90.1
Lobe affectation		
Higher	5	7.0
Middle or lingula	5	7.0
Lower	31	43.6
All	30	42.2
Distribution		
Subpleural	61	85.9
Patches	6	8.4
Peribronchovascular (central)	4	5.6
Other findings		
Subpleural lines	25	35.2
Adenopathies	20	28.1
Fibrosis	13	18.3
Pleural effusion	11	15.4
Reversed "halo sign"	2	2.8
Degree of lung involvement by tomography		
CT score mild	20	28.1
CT score moderate	28	39.4
CT score severe	23	32.3

Note. Data in parentheses are percentages.
Source: Authors' own elaboration.

The degree of involvement using the semi-quantitative measurement of the extent of lesions by pulmonary lobes was classified into mild involvement (62.7%), moderate involvement (21.5%), and severe involvement (15.6%). GGO was significantly more prevalent in mild (15 patients, 21.1%, $p < 0.001$) compared to moderate (nine patients, 12.6%) and severe (one patient, 1.4%), while pulmonary consolidation patterns (four patients, 5.6%; $p < 0.048$) and crazy paving and fibrosis (eight patients, 11.2%, $p < 0.033$) were significantly more common in severe affectation. There were no significant differences for the inverted halo sign, pleural effusion, and lymphadenopathy in terms of the degree of involvement (Table 3).

ACTA UNIVERSITARIA
Multidisciplinary Scientific Journal

ISSN online 2007-9621
García-Alvarado, F. J., Muñoz Hernández, M. A.,Segura Lopez, F. K., Delgado-Aguirre, H. A. Gaona Hernández, Y. A., & Arellano Rosales, J. S.
Lung involvement by chest CT images in covid-19 patients in a Specialty Hospital in the Northeast of Mexico | 1-12

Table 3. Characteristics of the chest tomography and the degree of pulmonary involvement of the covid-19 disease.

CT features in SARS-CoV-2+ patients	mild affectation n = 20	moderate affectation n = 28	severe affectation n = 23	p value
Chest CT scan	CT score 1 a 5	CT score >5 a 15	CT score >15	
Ground glass opacity	15 (21.1)	9 (12.6)	1 (1.4)	*0.001*
Crazy paving	1 (1.4)	8 (11.2)	6 (8.4)	0.111
Consolidation	0	1 (1.4)	4 (5.6)	*0.048*
Subpleural lines	11 (15.4)	7 (9.8)	7 (9.8)	0.084
Reversed "halo sign"	0	2 (2.8)	0	0.206
Adenopathies	3 (4.2)	11 (15.4)	6 (8.4)	0.176
Fibrosis	1 (1.4)	4 (5.6)	8 (11.2)	*0.033*

Note. Chi-square test (χ^2).
Source: Authors' own elaboration.

The characteristics of the chest tomography and the clinical classification of covid-19 according to the severity of the symptoms in this group of patients was that the GGO tomographic pattern was significantly more prevalent in the mild clinical stage (19 patients, 26.7%; p <0.001), while the crazy paving tomographic pattern (15 patients, 21.1%; p < 0.001) in the moderate clinical stage and pulmonary consolidation (three patients, 4.2%; p < 0.003) were significantly more frequent in the severe clinical stage of this group of patients (Table 4).

Table 4. Characteristics of the chest tomography and covid-19 clinical classification according to symptom severity.

CT features in SARS-CoV-2+ patients	mild stage n = 21	moderate stage n = 41	severe stage n = 9	p value
Ground glass opacity	19 (26.7)	6 (8.4)	0 (0)	*0.001*
Crazy paving	0	15 (21.1)	0	*0.001*
Consolidation	0	2 (2.8)	3 (4.2)	*0.003*
Subpleural lines	11 (15.4)	12 (16.9)	2 (2.8)	0.134
Reversed "halo sign"	0	1 (1.4)	1 (1.4)	0.236
Adenopathies	12 (16.9)	15 (21.1)	3 (4.2)	0.076
Fibrosis	2 (2.8)	9 (12.6)	2 (2.8)	0.463

Note. Chi-square test (χ^2).
Source: Authors' own elaboration.

Discussion

Among the tomographic findings by covid-19 (as mentioned in the present study) was the existence of bilateral GGO with mixed areas and pulmonary consolidation, predominantly peripheral distribution by lower lobes; previous studies agree with these results (Simpson *et al.*, 2020; Zhou *et al.*, 2020). When contrasting our results with those described in the literature, we found that Pan *et al.* (2020) demonstrated that the tomographic findings were variable according to the evolution of the disease. Colombi *et al.* (2020) with a cohort of 236 patients indicated that the level of lung involvement by CT and death or admission to the intensive care unit are positively correlated. A recent study used metrics with the combination of demographic parameters, CT metrics, and laboratory findings to predict the management of covid-19 patients through automated image analysis (Weikert *et al.*, 2021). The high frequency of the GGO tomographic pattern observed in the mild disease involvement in the patient group can indicate a possible relationship between the acute phase diffuse alveolar damage and bronchiolar fibrin, airspace edema, and interstitial thickening (Li *et al.*, 2020b). The disease can progress late after activating virus-specific B and T cell-mediated humoral and cellular immunity, leading to an intense formation of pro-inflammatory cytokines, capable of triggering an uncontrolled autoimmune response. These results can indicate a high prevalence of local paving pattern, as well as pulmonary consolidation areas found in the studied severely affected patients, which possibly result from the blend of bacterial superinfection, edema, and inflammatory changes (Tian *et al.*, 2020).

The clinical course of covid-19 is highly unpredictable because its manifestations are heterogeneous, ranging from asymptomatic, subclinical, or even critical illness with ARDS or multi-organ failure. There is no good prognostic biomarker available to identify patients who require immediate medical attention and to estimate the number of deaths (Yuan *et al.*, 2020). Disease progression predicted by CT and its association with laboratory and clinical findings are possibly useful to help medical personnel classify patients and establish a good treatment that is effective. However, covid-19 is still treated merely based on empirical decisions rather than observations obtained from large clinical trials (Rubin *et al.*, 2020). Like the group of Francone *et al.* (2020), the previously validated CT score was used according to the lobar extension of the disease as declared by Pan *et al.* (2020), whoagreed with some findings in evaluating this scale.

The diagnostic role of chest CT remains controversial. Although several researchers and radiological societies do not recommend using CT as a firstling test (Choi *et al.*, 2020; Li *et al.*, 2020a), the current study seems to suggest that an imaging method such as chest tomography could be of great help for physicians to have a better quantitative evaluation of CT images and a better clinical classification of the disease by covid-19, and thus accelerating diagnostic and therapeutic workflow.

The sensitivity and specificity of the chest CT in diagnosing covid-19 and the radiation exposure should be judged together (Kovács *et al.*, 2020). Chest CT in patients with typical clinical symptoms in highly infected regions or with close contact of covid-19-infected patients who had negative RT-PCR result is warranted. In a recent meta-analysis, Zheng *et al.* (2020) found that GGO, vascular enlargement, interlobular septal thickening, and subpleural bands were the most common findings in either common or severe patients. Compared to those of common patients, some CT manifestations were more frequent in severe patients, such as traction bronchiectasis, interlobular septal thickening, pulmonary consolidation, crazy-paving pattern, reticulation, pleural effusion, and lymphadenopathy. In this study, the assessment of inter- and intra-observer concordance was not carried out, so it is important to take into account this factor to reduce possible biases.

The present retrospective study faced some limitations. It was performed on a relatively small cohort of patients; therefore, it is suggested that future studies could be performed using a larger sample size and longer follow-up. The studied specialty hospital (UMAE N° 71) is considered a referral center for covid-19 patients; therefore, the total CT score of our patients cannot represent the general population.

Conclusions

In conclusion, we present the tomographic results of patients referring to a specialty hospital, with lung involvement due to covid-19, who had GGO and a mixed peripheral pattern toward the posterior regions. Tomographic features of lung lesions regarding subpleural and bilateral distribution showed that the lower lobes were more involved. The degree of involvement using semi-quantitative (CT-score) measurement of the extent of lesions by pulmonary lobes was classified in a higher proportion as moderate affectation.

Conflicts of interest

The authors declare that there is not conflict of interest.

References

Ai, T., Yang, Z., Hou, H., Zhan, C., Chen, C., Lv, W., Tao, Q., Sun, Z., & Xia, L. (2020). Correlation of chest CT and RT-PCR testing for coronavirus disease 2019 (covid-19) in China: A report of 1014 cases. *Radiology, 296*(2), 32-40. doi: https://doi.org/10.1148/radiol.2020200642

Bernheim, A., Mei, X., Huang, M., Yang, Y., Fayad, Z. A., Zhang, N., Diao, K., Lin, B., Zhu, X., Li, K., Li, S., Shan, H., Jacobi, A., & Chung, M. (2020). Chest CT findings in coronavirus disease-19 (covid-19): Relationship to duration of infection. *Radiology, 295*(3), 685-691. doi: https://doi.org/10.1148/radiol.2020200463

Colombi, D., Bodini, F. C., Petrini, M., Maffi, G., Morelli, N., Milanese, G., Silva, M., Sverzellati, N., & Michieletti, E. (2020). Well-aerated lung on admitting chest CT to predict adverse outcome in covid-19 pneumonia. *Radiology, 296*(2), 86-96. doi: https://doi.org/10.1148/radiol.2020201433

Choi, A. D., Abbara, S., Branch, K. R., Feuchtner, G. M., Ghoshhajra, B., Nieman, K., Pontone, G., Villines, T. C., Williams, M. C., & Blankstein, R. (2020). Society of Cardiovascular Computed Tomography guidance for use of cardiac computed tomography amidst the covid-19 pandemic endorsed by the American College of Cardiology. *Journal of Cardiovascular Computed Tomography, 14*(2), 101–104.
doi: https://doi.org/10.1016/j.jcct.2020.03.002

Chung, M., Bernheim, A., Mei, X., Zhang, N., Huang, M., Zeng, X., Cui, J., Xu, W., Yang, Y., Fayad, Z. A., Jacobi, A., Li, K., Li, S., & Shan, H. (2020). CT imaging features of 2019 novel coronavirus (2019-nCoV). *Radiology, 295*(1), 202–207. doi: https://doi.org/10.1148/radiol.2020200230

Francone, M., Iafrate, F., Masci, G. M., Coco, S., Cilia, F., Manganaro, L., Panebianco, V., Andreoli, C., Colaiacomo, M. C., Zingaropoli, M. A., Ciardi, M. R., Mastroianni, C. M., Pugliese, F., Alessandri, F., Turriziani, O., Ricci, P., & Catalano, C. (2020). Chest CT score in covid-19 patients: Correlation with disease severity and short-term prognosis. *European Radiology, 30*, 6808–6817. doi: https://doi.org/10.1007/s00330-020-07033-y

Hansell, D. M., Bankier, A. A., MacMahon, H., McLoud, T. C., Müller, N. L., & Remy, J. (2008). Fleischner society: Glossary of terms for thoracic imaging. *Radiology, 246*(3), 697–722.
doi: https://doi.org/10.1148/radiol.2462070712

Jiang, Z., He, C., Wang, D., Shen, H., Sun, J., Gan, W., Lu, J., & Liu, X. (2020). The role of imaging techniques in management of covid-19 in China: From diagnosis to monitoring and follow-up. *Medical Science Monitor, 26*, e924582. doi: https://doi.org/10.12659/msm.924582

Kovács, A., Palásti, P., Veréb, D., Bozsik, B., Palkó, A., & Kincses, Z. T. (2020). The sensitivity and specificity of chest CT in the diagnosis of covid-19. *European Radiology*, *31*(5), 2819–2824.
doi: https://doi.org/10.1007/s00330-020-07347-x

Li, K., Fang, Y., Li, W., Pan, C., Qin, P., Zhong, Y., Liu, X., Huang, M., Liao, Y., & Li, S. (2020a). CT image visual quantitative evaluation and clinical classification of coronavirus disease (covid-19). *European Radiology, 30*(8), 4407–4416. doi: https://doi.org/10.1007/s00330-020-06817-6

Li, X., Geng, M., Peng, Y., Meng, L., & Lu, S. (2020b). Molecular immune pathogenesis and diagnosis of covid-19. *Journal of Pharmaceutical Analysis, 10*(2), 102–108. doi: https://doi.org/10.1016/j.jpha.2020.03.001

Ooi, G. C., Khong, P. L., Müller, N. L., Yiu, W. C., Zhou, L. J., Ho, J. C. M., Lam, B., Nicolaou, S., & Tsang, K. W. T. (2004). Severe acute respiratory syndrome: Temporal lung changes at thin-section CT in 30 patients. *Radiology, 230*(3), 836–844. doi: https://doi.org/10.1148/radiol.2303030853

Pan, F., Ye, T., Sun, P., Gui, S., Liang, B., Li, L., Zheng, D., Wang, J., Hesketh, R. L., Yang, L., & Zheng, C. (2020). Time course of lung changes at chest CT during recovery from coronavirus disease 2019 (covid-19). *Radiology, 295*(3), 715–721. doi: https://doi.org/10.1148/radiol.2020200370

Prokop, M., van Everdingen, W., van Rees, T., Quarles, H., Stöger, L., Beenen, L., Geurts, B., Gietema, H., Krdzalic, J., Schaefer-Prokop, C., van Ginneken, B., & Brink, M. (2020). CO-RADS: A categorical CT assessment scheme for patients suspected of having covid-19—definition and evaluation. *Radiology, 296*(2), 97-104. doi: https://doi.org/10.1148/radiol.2020201473

Rubin, E. J., Harrington, D. P., Hogan, J. W., Gatsonis, C., Baden, L. R., & Hamel, M. B. (2020). The urgency of care during the Covid-19 Pandemic — Learning as we go. *New England Journal of Medicine, 382*(25), 2461–2462. doi: https://doi.org/10.1056/nejme2015903

Sánchez-Duque, J. A., Arce-Villalobos, L. R., & Rodríguez-Morales, A. J. (2020). Enfermedad por coronavirus 2019 (covid-19) en América Latina: Papel de la atención primaria en la preparación y respuesta. *Atención Primaria, 52*(6), 369–372. doi: https://doi.org/10.1016/j.aprim.2020.04.001

Simpson, S., Kay, F. U., Abbara, S., Bhalla, S., Chung, J. H., Chung, M., Henry, T. S., Kanne, J. P., Kligerman, S., Ko, J. P., & Litt, H. (2020). Radiological Society of North America Expert Consensus Document on reporting chest CT findings related to covid-19: Endorsed by the Society of Thoracic Radiology, the American College of Radiology, and RSNA. *Radiology: Cardiothoracic Imaging, 2*(2), e200152. doi: https://doi.org/10.1148/ryct.2020200152

Suárez, V., Suarez-Quezada, M., Oros-Ruiz, S., & Ronquillo, E. (2020). Epidemiología de covid-19 en México: Del 27 de febrero al 30 de abril de 2020. *Revista Clínica Española, 220*(8), 463–471. doi: https://doi.org/10.1016/j.rce.2020.05.007

Tian, S., Xiong, Y., Liu, H., Niu, L., Guo, J., Liao, M., & Xiao, S. (2020). Pathological study of the 2019 novel coronavirus disease (covid-19) through postmortem core biopsies. *Modern Pathology, 33*(6), 1007–1014. doi: https://doi.org/10.1038/s41379-020-0536-x

Wang, D., Hu, B., Hu, C., Zhu, F., Liu, X., Zhang, J., Wang, B., Xiang, H., Cheng, Z., Xiong, Y., Zhao, Y., Li, Y., Wang, X., & Peng, Z. (2020). Clinical characteristics of 138 hospitalized patients with 2019 novel coronavirus–infected pneumonia in Wuhan, China. *JAMA, 323*(11), 1061-1069. doi: https://doi.org/10.1001/jama.2020.1585

Weikert, T., Rapaka, S., Grbic, S., Re, T., Chaganti, S., Winkel, D. J., Anastasopoulos, C., Niemann, T., Wiggli, B. J., Bremerich, J., Twerenbold, R., Sommer, G., Comaniciu, D., & Sauter, A. W. (2021). Prediction of patient management in covid-19 using deep learning-based fully automated extraction of cardiothoracic CT metrics and laboratory findings. *Korean Journal of Radiology, 22*(6), 994-1004. doi: https://doi.org/10.3348/kjr.2020.0994

World Health Organization (WHO). (2020a). *Coronavirus disease 2019 (covid-19): Situation report, 82*. https://apps.who.int/iris/handle/10665/331780

World Health Organization (WHO). (2020b). *Global surveillance for covid-19 caused by human infection with covid-19 virus: Interim guidance, 20 March 2020*. https://apps.who.int/iris/handle/10665/331506

Wu, Z., & McGoogan, J. M. (2020). Characteristics of and important lessons from the coronavirus disease 2019 (covid-19) outbreak in China. *JAMA, 323*(13), 1239-1242. doi: https://doi.org/10.1001/jama.2020.2648

Yuan, Y., Goncalves, J., Xiao, Y., Zhang, H., Xu, H., & Cao, Z. (2020). Reply to: Clinical interpretation of an interpretable prognostic model for patients with covid-19. *Nature Machine Intelligence, 3*(2020). doi: https://doi.org/10.1038/s42256-020-0206-1

Zheng, Y., Wang, L., & Ben, S. (2020). Meta-analysis of chest CT features of patients with covid-19 pneumonia. *Journal of Medical Virology*, *93*(1), 241–249. doi: https://doi.org/10.1002/jmv.26218

Zhou, S., Wang, Y., Zhu, T., & Xia, L. (2020). CT features of coronavirus disease 2019 (covid-19) pneumonia in 62 patients in Wuhan, China. *American Journal of Roentgenology, 214*(6), 1287–1294. doi: https://doi.org/10.2214/ajr.20.22975

Zu, Z. Y., Jiang, M. D., Xu, P. P., Chen, W., Ni, Q. Q., Lu, G. M., & Zhang, L. J. (2020). Coronavirus disease 2019 (covid-19): A perspective from China. *Radiology, 296*(2), 15-25. doi: https://doi.org/10.1148/radiol.2020200490